Improving the isolation performance of seat suspension using negative stiffness cam-springs

Vanliem Nguyen[1], Trungkien Nguyen[2], Tronghoan Nguyen[3], Haianh Pham[4]
Faculty of Automotive Engineering Technology, Dai Nam University, Hanoi, Vietnam
[1]Corresponding author
E-mail: [1]*liemnv@dainam.edu.vn*, [2]*nguyentrungkien@dainam.edu.vn*, [3]*hoannt.cko@dainam.edu.vn*, [4]*anhph@dainam.edu.vn*

Received 13 May 2026; accepted 3 August 2026; published online 1 November 2026
DOI https://doi.org/10.21595/vp.2026.26668

78th International Conference on Vibroengineering in Lviv, Ukraine, October 1, 2026

Copyright © 2026 Vanliem Nguyen, et al. This is an open access article distributed under the Creative Commons Attribution License, which permits unrestricted use, distribution, and reproduction in any medium, provided the original work is properly cited.

Abstract. To further improve the isolation performance of the seat's suspension system of vehicles, this study proposes a new design of the negative stiffness using two cam-springs (NS-CS). To clarify the isolation performance of NS-CS, two different structures of the seat's traditional suspension (TS) and negative stiffness using the horizontal springs (NS-HS) are also used to compare the isolation performance between TS, NS-HS, and NS-CS. The performance indicators are evaluated through the seat's acceleration in the time region and the seat's power spectral density acceleration in the frequency region. The study shows that both these indices with NS-CS are lower than those of TS and NS-HS. Thus, the proposed NS-CS model improves driver's comfort more than NS-HS.

Keywords: seat's suspension, negative stiffness (NS), NS-HS, NS-CS, driver's comfort.

1. Introduction

To improve the vehicle's ride comfort, suspension systems have been widely optimized and controlled [1-4]. The comfort performance of vehicles has been significantly improved. However, the acceleration of the driver's seat remains high when vehicles travel on poor road surfaces, especially in heavy trucks and construction vehicles. To solve this issue, the seat's suspension in these vehicles has been extensively studied and controlled using advanced control methods [5-9]. These methods have improved driver comfort by up to 35 % compared to passive seat suspensions. However, the disadvantage of the seat's control suspension system is its high cost. Therefore, researchers are actively developing a passive seat suspension system that incorporates negative stiffness (NS) to improve seat comfort [10-12]. Existing studies show that the structure of NS is simple, but its vibration isolation efficiency is very high.

Based on this isolation efficiency of NS, different structures of NS using air pistons, curved-roller springs, and negative dampers were developed to optimize the seat's suspension system [13-15]. The study results indicate that the geometric parameters of the NS greatly influence its isolation effectiveness. However, the studies have revealed that the structure of NS, with its highly nonlinear characteristics, is capable of better vibration isolation than other simpler NS structures. Therefore, based on the initial design of NS-HS (NS using two horizontal springs) added to the seat's suspension system, this study proposes a new design of the NS using cam-springs (NS-CS) to enhance the isolation performance of the seat suspension system as well as further improve the driver's comfort.

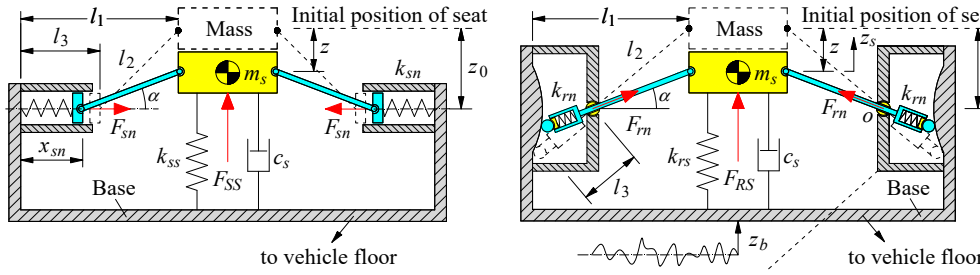
2. Mathematical models of NS-HS and NS-CS

NS-HS model: The model of NS-HS has been designed and applied in existing studies [10, 11]. Its structure includes two horizontal springs of the negative stiffness structures added to the seat's traditional suspension (TS), as shown in Fig. 1(a). Here, l_1, l_2, and l_3 are the initial distances between the seat and the base wall, bar length, and initial length of the horizontal spring;

m_s, k_{ss}, and c_s are the mass, stiffness, and damping values of the seat and the TS; F_{sn} and F_{ss} are the restoring forces of the NS-HS and the seat's TS added by NS-HS; z_0 and z are the seat's initial position and dynamic displacement of the system.

In the case of the standard seat's TS without NS-HS, the force response of the seat's TS is:

$$F_{TS} = k_{ss}z + c_s\dot{z}. \tag{1}$$



a) Model of NS-HS b) Model of NS-CS

Fig. 1. Models of the seat suspension system

When the seat's TS is added by NS-HS, the force response of NS-HS is written as [11]:

$$F_{NS-HS} = F_{SS} = k_{ss}z + c_s\dot{z} + 2k_{sn}\frac{l_3 - x_{sn}}{l_1 - x_{sn}}(z_0 - z), \tag{2}$$

where $x_{sn} = l_1 - \text{sqrt}[l_2^2 - (z_0 - z)^2]$ and $z_0 = \text{sqrt}[l_2^2 - (l_1 - l_3)^2]$.

To evaluate the characteristics of the seat's NS-HS, the non-dimensional equation between the restoring force and displacement needs to be derived. Based on constant values of k_{ss} and l_1, and neglecting the effect of the damper ($c_s = 0$), dividing Eq. (2) by ($k_{ss} \times l_1$), we have:

$$\frac{F_{NS-HS}}{k_{ss}l_1} = \frac{z}{l_1} + 2\frac{k_{sn}}{k_{ss}}\frac{l_3 - x_{sn}}{l_1 - x_{sn}}\left(\frac{z_0}{l_1} - \frac{z}{l_1}\right). \tag{3}$$

Let $\bar{F}_{NS-HS} = \frac{F_{NS-HS}}{k_{ss}l_1}$, $\bar{z} = \frac{z}{l_1}$, $\bar{z} = \frac{z}{l_1}$, $\bar{z}_0 = \frac{z_0}{l_1}$, $\alpha_1 = \frac{l_2}{l_1}$, $\alpha_2 = \frac{l_3}{l_1}$, $\beta = \frac{k_{sn}}{k_{ss}}$, the non-dimensional equation used to describe the restoring force-displacement characteristics is written as:

$$\bar{F}_{NS-HS} = \bar{z} + 2\beta\left(1 + \frac{\alpha_2 - 1}{\text{sqrt}[\alpha_1^2 - (\bar{z}_0 - \bar{z})^2]}\right)(\bar{z}_0 - \bar{z}), \tag{4}$$

where α_1 and α_2 are defined as the geometric dimension ratios of NS-HS, while β is defined as the stiffness ratio of NS-HS. These ratios greatly affect the isolation performance of NS-HS. Thus, they need to be optimized to enhance this effectiveness.

NS-CS model: Based on the model of NS-HS, two horizontal springs of the negative stiffness structures are replaced by the cam-spring (NS-CS), as shown in Fig. 1(b). Here, the symbols in Fig. 1(b) are the same as in Fig. 1(a).

Under the effect of the mass of the driver's seat, the seat's displacement is z; thus, the force response of the seat's NS-CS is calculated as follows:

$$F_{NS-CS} = F_{RS} = k_{rs}z + c_s\dot{z} + 2k_{rn}\frac{l_3 - x_{rn}}{\text{sqrt}[(l_2^2 - z_0^2) + (z_0 - z)^2]}(z_0 - z). \tag{5}$$

From the NS-CS's geometrical dimension described in Fig. 1(b), Eq. (5) is rewritten by:

$$F_{NS-CS} = k_{rs}\mathrm{z} + c_s\dot{z} + 2k_{rn}\left(l - \frac{(l_0 + l_1)Z_1}{\sqrt{l_2^2 - z_0^2}} + \frac{Z_2}{\sqrt{l_2^2 - z_0^2}}\right)\frac{z_0 - z}{Z_1}, \quad (6)$$

where $Z_1 = sqrt[(l_2^2 - z_0^2) + (z_0 - z)^2]$, $Z_2 = sqrt[(R + r)^2 Z_1^2 - (l_3 - r)^2(z_0 - z)^2]$, R is the curved wall's radius, and r is the roller radius, and $l = r + l_2 + l_3$.

Similarly, to evaluate the characteristics of the seat's NS-CS, the non-dimensional equation between the restoring force and displacement also needs to be derived. Thus, based on constant values of k_{rs} and l_1, and ignoring the effect of c_s, dividing Eq. (6) by $(k_{rs} \times l_1)$, we have:

$$\bar{F}_{NS-CS} = \bar{z} + 2\beta\left(\alpha - \frac{(\gamma_5 + 1)\bar{Z}_1}{\sqrt{\gamma_1^2 - \bar{z}_0^2}} + \frac{\bar{Z}_2}{\sqrt{\alpha_1^2 - \bar{z}_0^2}}\right)\frac{\bar{z}_0 - \bar{z}}{\bar{Z}_1}, \quad (7)$$

where $\bar{F}_{NS-CS} = \frac{F_{NS-CS}}{k_{ss}l_1}$, $\bar{z} = \frac{z}{l_1}$, $\bar{z} = \frac{z}{l_1}$, $\bar{z}_0 = \frac{z_0}{l_1}$, $\alpha_1 = \frac{l_2}{l_1}$, $\alpha_2 = \frac{l_3}{l_1}$, $\alpha_3 = \frac{r}{l_1}$, $\alpha_4 = \frac{R}{l_1}$, $\alpha_5 = \frac{l_0}{l_1}$, $\alpha = \alpha_1 + \alpha_2 + \alpha_3$, $\beta = \frac{k_{rn}}{k_{ss}}$, $\bar{Z}_1 = \mathrm{sqrt}[(\gamma_1^2 - \bar{z}_0^2) + (\bar{z}_0 - \bar{z})^2]$, and $\bar{Z}_2 = [(\alpha_3 + \alpha_4)^2\bar{Z}_1^2 - (\alpha_2 - \alpha_3)^2(\bar{z}_0 - \bar{z})^2]$, respectively.

The ratios of α_{1-5} and β in the seat's NS-CS can also greatly affect the isolation performance of NS-CS. Thus, they also need to be optimized to enhance the isolation performance of NS-CS.

Excitation source of two models: The seat suspension system is used to isolate vibrations from the vehicle or cab's floor transmitting to the driver when the vehicle is moving on the road surface. Under actual condition of vehicles, the road surface is typically a random road excitation. Thus, this random road surface was mainly used as the input excitation of the vehicle models. To build the random excitation of the road surface, ISO-8608 [16] was applied in the existing research [10, 13-15]. Based on these study results, a type of random road surface in ISO level B built when the vehicle was traveling at a speed of 72 km/h was applied in this study to simulate the seat suspension system, as shown in Fig. 2(a).

3. Results and discussions

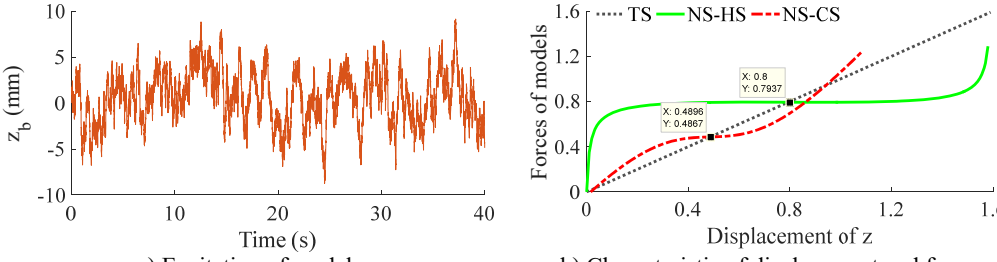
Evaluation index: The primary function of the seat suspension system is to isolate the driver's vibrations from road surface disturbances, thereby enhancing driver comfort. Based on ISO 2631-1 [17], the human comfort is evaluated by the root mean square value of the acceleration response of the human in the time domain, and this value is calculated by $a_{rms} = \sqrt{\frac{1}{T}\int_0^T a_s^2 dt}$. Here a_s is the acceleration response of the human (m/s^2), and T is the duration of the measurement or simulation. This value is commonly used to evaluate the driver comfort in the existing studies. In addition, human health is strongly affected by the vibration excitation in the low frequency region below 10 Hz. Existing research used the seat's power spectral density acceleration (PSD_{as}) in the frequency domain to evaluate human health [2-4, 9]. Therefore, the two indexes of a_{rms} and PSD_{as} are used to evaluate the isolation performance between the seat's TS, NS-HS, and NS-CS.

Based on the optimal ratios of $\{l_1, \alpha_1, \alpha_2, \text{and } \beta\}$ as well as the design parameters of the seat suspension in the existing studies [11], these parameters are then referenced and applied to both the NS-HS and NS-CS to study their performance. These parameters are listed in Table 1.

Table 1. The ratios and design parameters of the seat, NS-HS, and NS-CS

Parameters	Values	Parameters	Values	Parameters	Values
m_s (kg)	85	l_1 (mm)	261	α_3	0.14
c_s (Ns/m)	250	α_1	0.85	α_4	0.23
k_s (N/m)	47890	α_2	0.42	β	0.45

Characteristics of NS-HS and NS-CS: Under the same optimal parameters and ratios of the seat's suspension system using NS-HS and NS-CS in Table 1, the non-dimensional equations which describe the relationship between the restoring force and displacement of NS-HS in Eq. (4) and NS-CS in Eq. (7) are simulated and presented in Fig. 2(b).

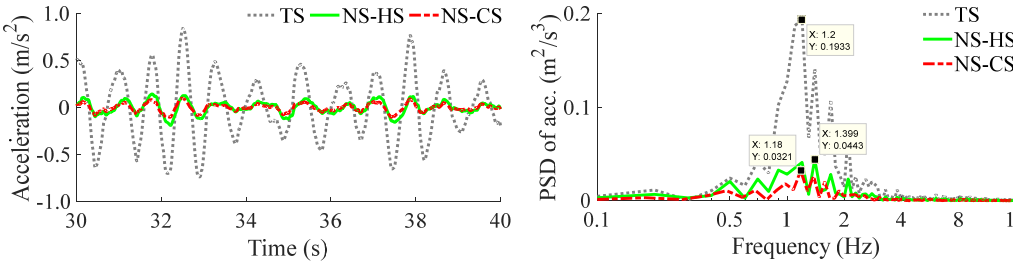


a) Excitation of models b) Characteristic of displacement and force

Fig. 2. Excitation source and force-displacement of models

For the seat's TS without the negative stiffness, the non-dimensional characteristic between the displacement and restoring force is linear. For the seat's NS-HS and NS-CS, under the effect of the negative stiffness added in these structures, their non-dimensional characteristics represent the relationship between the displacements and restoring forces, which are the non-linear curves. With NS-HS, when the displacement of z increases from 0.2 to 1.4, the restoring force changes insignificantly, indicating this is the stable region of NS-HS. Similarly for NS-CS, when the displacement of z increases from 0.3 to 0.7, the restoring force is insignificantly changed. Thus, this is the stable region of NS-CS. Within these stable regions, the restoring force value of the NS-CS is 0.486, while that of the NS-HS is 0.794. Thus, the restoring force value of NS-CS is smaller than that of NS-HS under the same deformation of the suspension system of the seat. Based on the relation $F = m_s \times a_s$, if the restoring force value of NS-CS (F_{NS-CS} in Eq. (5)) is smaller than the restoring force value of NS-HS (F_{NS-HS} in Eq. (2)), the acceleration a_s generated by F_{NS-CS} is also smaller than a_s generated by F_{NS-HS}. Thus, the isolation performance of NS-CS is better than that of NS-HS.

Comparing the isolation performance between NS-HS and NS-CS: Based on the analysis results of the non-dimensional characteristics of the NS-HS and NS-CS, the restoring force response generated by the NS-CS is smaller than that of the NS-HS. Under the same excitation from the vehicle or cab's floor defined by z_b as described in Fig. 1(b), the displacement of the seat suspension is $z = z_b - z_s$, while the displacement and acceleration of the driver's seat are defined by z_s and a_s. The simulation results of the seat's acceleration response and PSD_{as} for TS, NS-HS, and NS-CS are shown in Figs. 3(a) and 3(b). In addition, the a_{rms} and $PSD_{as,max}$ are computed and listed in Table 2.



a) Acceleration response b) PSD acceleration

Fig. 3. Seat's acceleration using NS-HS and NS-CS

Fig. 3 shows that both the acceleration and PSD acceleration of the driver's seat with TS are very high. With the NS-SH and NS-CS applied to the seat suspension system, both these values

are strongly decreased compared to the seat's TS. Thus, the driver's comfort is greatly improved with NS-SH and NS-CS. In addition, since the restoring force of NS-CS is smaller than that of NS-HS, the results of the acceleration and PSD acceleration of the driver's seat with NS-CS are smaller than those of NS-HS. The computed results in Table 2 show that the a_{rms} and $PSD_{as,max}$ values with NS-CS are reduced by 84.1 % and 83.4 % compared to TS; and reduced by 30.0 % and 27.4 % compared to NS-HS, respectively. This means that the NS-CS isolates the vibration of the seat's suspension system better than the NS-HS in both the working regions of time and frequency.

Table 2. The comparison results of a_{rms} and $PSD_{as,max}$

Parameters	TS	NS-HS	NS-CS	NS-CS versus TS	NS-CS versus NS-HS
a_{rms} (m/s^2)	0.44	0.10	0.07	84.1 %	30.0 %
$PSD_{as,max}$ (m^2/s^3)	0.193	0.044	0.032	83.4 %	27.4 %

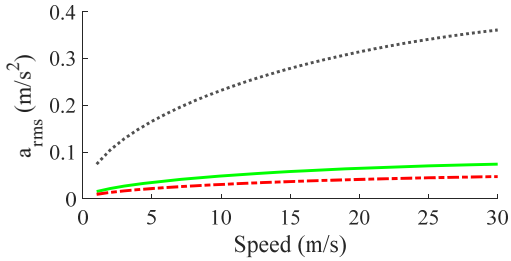


Fig. 4. The seat's acceleration under various speeds

The vehicle's moving speed could be changed when the vehicle is moving on the road surface, which could affect the isolation performance of NS-CS. Thus, the effect of the vehicle's speed on the NS-CS's stability is also simulated and presented in Fig. 4. Fig. 4 shows that the a_{rms} with TS is strongly increased with the increasing speed of the vehicle, while this value with NS-HS and NS-CS is insignificantly increased when the vehicle's speed is increased. Especially, the a_{rms} with NS-CS is insignificantly changed and remain smaller than both TS and NS-HS.

4. Conclusions

From the above study results, the isolation performance of the seat's TS is limited; thus, the driver's comfort is also poor.

With the NS-HS and NS-CS added to the seat suspension system, both the a_{rms} and $PSD_{as,max}$ values are substantially reduced compared to the TS. Besides, both these values with the NS-CS are smaller than those of the NS-HS under various simulations. Thus, under the same operating conditions of the vehicle, the NS-CS improves the driver's comfort more effectively than the NS-HS and TS.

The current study is limited to numerical simulation and the optimization of geometric ratios (alpha1 through alpha5) via sensitivity analysis. To fully evaluate the isolation performance of the NS-CS and apply it to different vehicles, as well as to physical test-rig validation, these studies are planned for future research.

Acknowledgements

The authors wish to thank the Dai Nam University for supporting this work.

Data availability

The datasets generated during and/or analyzed during the current study are available from the

corresponding author on reasonable request.

Conflict of interest

The authors declare that they have no conflict of interest.

References

[1] R. Pekgökgöz, M. Gürel, M. Bilgehan, and M. Kısa, "Active suspension of cars using fuzzy logic controller optimized by genetic algorithm," *International Journal of Engineering and Applied Sciences*, Vol. 2, No. 4, pp. 27–37, Dec. 2010.

[2] B. Su and C. Wang, "Efficiency and stability of heavy vehicle's control air suspensions on improving road friendliness and comfort level," *Noise and Vibration Worldwide*, Vol. 56, No. 10-11, pp. 594–607, Dec. 2025, https://doi.org/10.1177/09574565251359159

[3] T. Li, "Evaluation of damping characteristic and optimal design of cab's hydraulic mount in soil compactor," *Proceedings of the Institution of Mechanical Engineers, Part D: Journal of Automobile Engineering*, Vol. 240, No. 1, pp. 353–364, Jan. 2025, https://doi.org/10.1177/09544070251313650

[4] T. Li, "Analysis and optimization of the quadratic damping values of hydraulic dampers added in vibratory roller's cab isolations," *The International Journal of Acoustics and Vibration*, Vol. 30, No. 1, pp. 102–111, Mar. 2025, https://doi.org/10.20855/ijav.2025.30.12116

[5] V. Nguyen, R. Jiao, and J. Zhang, "Control performance of damping and air spring of heavy truck air suspension system with optimal fuzzy control," *Journal of Vehicle Dynamics, Stability, and NVH*, Vol. 4, No. 2, pp. 179–194, Feb. 2020, https://doi.org/10.4271/10-04-02-0013

[6] H. E. Tseng and D. Hrovat, "State of the art survey: active and semi-active suspension control," *Vehicle System Dynamics*, Vol. 53, No. 7, pp. 1034–1062, Jul. 2015, https://doi.org/10.1080/00423114.2015.1037313

[7] Z. Xie, P. K. Wong, J. Zhao, T. Xu, K. I. Wong, and H. C. Wong, "A noise-insensitive semi-active air suspension for heavy-duty vehicles with an integrated fuzzy-wheelbase preview control," *Mathematical Problems in Engineering*, Vol. 2013, pp. 1–12, Jul. 2013, https://doi.org/10.1155/2013/121953

[8] L. Ming, L. Yibin, R. Xuewen, Z. Shuaishuai, and Y. Yanfang, "Semi-active suspension control based on deep reinforcement learning," *IEEE Access*, Vol. 8, pp. 9978–9986, Jan. 2020, https://doi.org/10.1109/access.2020.2964116

[9] V. Nguyen, J. Zhang, V. Le, R. Jiao, and L. Xin, "Performance analysis of air suspension system of heavy truck with semi-active fuzzy control," (in Chinese), *Journal of Southeast University*, Vol. 33, No. 2, p. 159, Jul. 2017, https://doi.org/10.3969/j.issn.1003-7985.2017.02.006

[10] J. Zha, V. Nguyen, B. Su, R. Jiao, and D. Ni, "Performance of the seat suspension system using negative stiffness structure on improving the driver's ride comfort," *Journal of Vehicle Dynamics, Stability, and NVH*, Vol. 6, No. 2, pp. 135–146, Feb. 2022, https://doi.org/10.4271/10-06-02-0009

[11] J. Zha, V. Nguyen, D. Ni, and B. Su, "Optimizing the geometrical dimensions of the seat suspension equipped with a negative stiffness structure based on a genetic algorithm," *Journal of Vehicle Dynamics, Stability, and NVH*, Vol. 6, No. 2, pp. 147–158, Feb. 2022, https://doi.org/10.4271/10-06-02-0010

[12] H. Iemura and M. H. Pradono, "Advances in the development of pseudo-negative-stiffness dampers for seismic response control," *Structural Control and Health Monitoring*, Vol. 16, No. 7–8, Nov. 2009, https://doi.org/10.1002/stc.345

[13] L. Dong and R. Lakes, "Advanced damper with high stiffness and high hysteresis damping based on negative structural stiffness," *International Journal of Solids and Structures*, Vol. 50, No. 14-15, pp. 2416–2423, Apr. 2013, https://doi.org/10.1016/j.ijsolstr.2013.03.018

[14] D. Ni, N. van Liem, and S. Li, "Performance analysis of the seat suspension using different models of the optimal negative-stiffness-structures," *Proceedings of the Institution of Mechanical Engineers, Part D: Journal of Automobile Engineering*, Vol. 237, No. 6, pp. 1313–1326, Apr. 2022, https://doi.org/10.1177/09544070221091040

[15] E. Davoodi, P. Safarpour, M. Pourgholi, and M. Khazaee, "Design and evaluation of vibration reducing seat suspension based on negative stiffness structure," *Proceedings of the Institution of Mechanical Engineers, Part C: Journal of Mechanical Engineering Science*, Vol. 234, No. 21, pp. 4171–4189, Apr. 2020, https://doi.org/10.1177/0954406220921203

[16] "Mechanical vibration-road surface profiles – Reporting of measured data," International Organization for Standardization, Geneve, Switzerland, ISO 8608, 1995.

[17] "Mechanical vibration and shock – Evaluation of human exposure to whole body vibration – Part 1: General requirements," International Organization for Standardization, Geneve, Switzerland, ISO 2631-1, 1997.